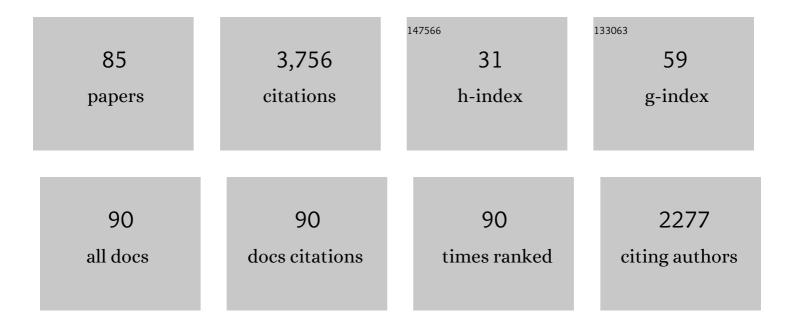
W Andy Take

List of Publications by Year in descending order

Source: https://exaly.com/author-pdf/6527405/publications.pdf Version: 2024-02-01



#	Article	IF	CITATIONS
1	A benchmarking study of four numerical runout models for the simulation of tailings flows. Science of the Total Environment, 2022, 827, 154245.	3.9	10
2	Evaluation of Shape Array sensors to quantify the spatial distribution and seasonal rate of track settlement. Transportation Geotechnics, 2021, 27, 100487.	2.0	2
3	Numerical simulation of impulse wave generation by idealized landslides with OpenFOAM. Coastal Engineering, 2021, 165, 103815.	1.7	24
4	Stability of saturated granular columns: Role of stress-dilatancy and capillarity. Physics of Fluids, 2021, 33, .	1.6	9
5	An efficient two-layer landslide-tsunami numerical model: effects of momentum transfer validated with physical experiments of waves generated by granular landslides. Natural Hazards and Earth System Sciences, 2021, 21, 1229-1245.	1.5	4
6	Catastrophic mass flows resulting from tailings impoundment failures. Engineering Geology, 2021, 292, 106262.	2.9	40
7	Geotechnical centrifuge modelling of retrogressive sensitive clay landslides. Canadian Geotechnical Journal, 2021, 58, 1452-1465.	1.4	15
8	The influence of image analysis methodology on the calculation of granular temperature for granular flows. Granular Matter, 2021, 23, 1.	1.1	5
9	Effect of Upstream Dam Geometry on Peak Discharge During Overtopping Breach in Noncohesive Homogeneous Embankment Dams; Implications for Tailings Dams. Water Resources Research, 2021, 57, .	1.7	6
10	Bridge transition monitoring: Interpretation of track defects using digital image correlation and distributed fiber optic strain sensing. Proceedings of the Institution of Mechanical Engineers, Part F: Journal of Rail and Rapid Transit, 2020, 234, 616-637.	1.3	9
11	Calculation of 3D displacement and time to failure of an earth dam using DIC analysis of hillshade images derived from high temporal resolution point cloud data. Landslides, 2020, 17, 499-515.	2.7	12
12	Simulations of Landslide Wave Generation and Propagation Using the Particle Finite Element Method. Journal of Geophysical Research: Oceans, 2020, 125, e2019JC015873.	1.0	36
13	Wave Generation Across a Continuum of Landslide Conditions From the Collapse of Partially Submerged to Fully Submerged Granular Columns. Journal of Geophysical Research: Oceans, 2020, 125, e2020JC016465.	1.0	18
14	Tailings-flow runout analysis: examining the applicability of a semi-physical area–volume relationship using a novel database. Natural Hazards and Earth System Sciences, 2020, 20, 3425-3438.	1.5	15
15	Non-Hydrostatic Modeling of Waves Generated by Landslides with Different Mobility. Journal of Marine Science and Engineering, 2019, 7, 266.	1.2	3
16	Instability of loose dry granular slopes observed in centrifuge tilting table tests. Geotechnique Letters, 2019, 9, 147-153.	0.6	3
17	Full scale investigation of GCL damage mechanisms in small earth dam retrofit applications under earthquake loading. Geotextiles and Geomembranes, 2019, 47, 502-513.	2.3	16
18	An Enhanced Framework to Quantify the Shape of Impulse Waves Using Asymmetry. Journal of Geophysical Research: Oceans, 2019, 124, 652-666.	1.0	13

#	Article	IF	CITATIONS
19	TXT-tool 3.044-1.1: The Runout of Chalk Cliff Collapses—Case Studies and Physical Model Experiments. , 2018, , 297-314.		1
20	Correlation of acoustic emissions with patterns of movement in an extremely slow-moving landslide at Peace River, Alberta, Canada. Canadian Geotechnical Journal, 2018, 55, 1475-1488.	1.4	29
21	Numerical modeling of normal fault-pipeline interaction and comparison with centrifuge tests. Soil Dynamics and Earthquake Engineering, 2018, 105, 127-138.	1.9	54
22	Field performance of a peat railway subgrade reinforced with helical screw piles. Canadian Geotechnical Journal, 2018, 55, 1888-1899.	1.4	10
23	Distributed fibre optic sensing of strains on buried full-scale PVC pipelines crossing a normal fault. Geotechnique, 2018, 68, 1-17.	2.2	100
24	Measurement of distributed dynamic rail strains using a Rayleigh backscatter based fiber optic sensor: Lab and field evaluation. Transportation Geotechnics, 2018, 14, 70-80.	2.0	31
25	Field measurements of overlap reductions for two reinforced fabric-encased geosynthetic clay liners (GCLs). Canadian Geotechnical Journal, 2018, 55, 631-639.	1.4	13
26	Reductions in GCL Overlap Beneath an Exposed Geomembrane. Journal of Geotechnical and Geoenvironmental Engineering - ASCE, 2018, 144, 04018094.	1.5	9
27	Dynamic measurements using digital image correlation. International Journal of Physical Modelling in Geotechnics, 2017, 17, 41-52.	0.5	8
28	On the transfer of momentum from a granular landslide to a water wave. Coastal Engineering, 2017, 125, 16-22.	1.7	45
29	Comparison of Wrinkles in White and Black HDPE Geomembranes. Journal of Geotechnical and Geoenvironmental Engineering - ASCE, 2017, 143, .	1.5	8
30	Tsunamis generated by long and thin granular landslides in a large flume. Journal of Geophysical Research: Oceans, 2017, 122, 653-668.	1.0	55
31	Performance assessment of peat rail subgrade before and after mass stabilization. Canadian Geotechnical Journal, 2017, 54, 674-689.	1.4	32
32	Measuring displacements of a railroad bridge using DIC and accelerometers. Smart Structures and Systems, 2017, 19, 225-236.	1.9	15
33	Measuring Crack Movement in Reinforced Concrete Using Digital Image Correlation: Overview and Application to Shear Slip Measurements. Proceedings of the IEEE, 2016, 104, 1561-1574.	16.4	34
34	Measurement of rail deflection on soft subgrades using DIC. Proceedings of the Institution of Civil Engineers: Geotechnical Engineering, 2016, 169, 383-398.	0.9	16
35	Response of pipelines of differing flexural stiffness to normal faulting. Geotechnique, 2016, 66, 275-286.	2.2	89
36	Effect of geomembrane colour and cover soil on solar-driven down-slope bentonite erosion from a GCL. Geosynthetics International, 2016, 23, 257-270.	1.5	14

#	Article	lF	CITATIONS
37	Effect of GCL Type on Downslope Erosion in an Exposed Composite Liner. Journal of Geotechnical and Geoenvironmental Engineering - ASCE, 2016, 142, .	1.5	24
38	Field and laboratory observations of down-slope bentonite migration in exposed composite liners. Geotextiles and Geomembranes, 2016, 44, 686-706.	2.3	32
39	Loss of slope support due to base liquefaction: comparison of 1g and centrifuge landslide flume experiments. Soils and Foundations, 2016, 56, 251-264.	1.3	11
40	Physical modelling of rainfall-induced flow failures in loose granular soils. IOP Conference Series: Earth and Environmental Science, 2015, 26, 012001.	0.2	0
41	Observations of grain-scale interactions and simulation of dry granular flows in a large-scale flume. Canadian Geotechnical Journal, 2015, 52, 638-655.	1.4	38
42	Thirty-Sixth Canadian Geotechnical Colloquium: Advances in visualization of geotechnical processes through digital image correlation. Canadian Geotechnical Journal, 2015, 52, 1199-1220.	1.4	117
43	Post-failure fracture angle of brittle pipes subjected to differential ground movements. Tunnelling and Underground Space Technology, 2015, 49, 114-120.	3.0	15
44	Influence of slope inclination on the triggering and distal reach of hydraulically-induced flow slides. Engineering Geology, 2015, 187, 170-182.	2.9	12
45	The runout of chalk cliff collapses in England and France—case studies and physical model experiments. Landslides, 2015, 12, 225-239.	2.7	18
46	Measurement of vertical and longitudinal rail displacements using digital image correlation. Canadian Geotechnical Journal, 2015, 52, 141-155.	1.4	62
47	Field monitoring of a bridge using digital image correlation. Proceedings of the Institution of Civil Engineers: Bridge Engineering, 2015, 168, 3-12.	0.3	18
48	Laboratory Study of Downslope Erosion for 10 Different GCLs. Journal of Geotechnical and Geoenvironmental Engineering - ASCE, 2015, 141, .	1.5	15
49	Effect of antecedent groundwater conditions on the triggering of static liquefaction landslides. Landslides, 2015, 12, 469-479.	2.7	40
50	Quantification of Optical Clarity of Transparent Soil Using the Modulation Transfer Function. Geotechnical Testing Journal, 2015, 38, 20140216.	0.5	17
51	Base liquefaction: a mechanism for shear-induced failure of loose granular slopes. Canadian Geotechnical Journal, 2014, 51, 496-507.	1.4	38
52	Factors affecting the down-slope erosion of bentonite in a GCL. Geotextiles and Geomembranes, 2014, 42, 445-456.	2.3	26
53	Laboratory Simulation of Bentonite Erosion by Downslope Flow on a GCL. Journal of Geotechnical and Geoenvironmental Engineering - ASCE, 2014, 140, .	1,5	16
54	Curvature Monitoring of Beams Using Digital Image Correlation. Journal of Bridge Engineering, 2014, 19, .	1.4	38

#	Article	IF	CITATIONS
55	Experimental Test of Theory for the Stability of Partially Saturated Vertical Cut Slopes. Journal of Geotechnical and Geoenvironmental Engineering - ASCE, 2014, 140, .	1.5	14
56	Comparison of confined and unconfined infiltration in transparent porous media. Water Resources Research, 2013, 49, 851-863.	1.7	32
57	Experimental accuracy of two dimensional strain measurements using Digital Image Correlation. Engineering Structures, 2013, 46, 718-726.	2.6	102
58	Large-Scale Quantification of Wrinkles in a Smooth Black HDPE Geomembrane. Journal of Geotechnical and Geoenvironmental Engineering - ASCE, 2012, 138, 671-679.	1.5	46
59	Time-dependent behaviour of the Bearpaw Shale in oedometric loading and unloading. Canadian Geotechnical Journal, 2012, 49, 427-441.	1.4	23
60	Optimum Accuracy of Two-Dimensional Strain Measurements Using Digital Image Correlation. Journal of Computing in Civil Engineering, 2012, 26, 795-803.	2.5	35
61	Thermal Expansion and Contraction of Geomembrane Liners Subjected to Solar Exposure and Backfilling. Journal of Geotechnical and Geoenvironmental Engineering - ASCE, 2012, 138, 1387-1397.	1.5	27
62	Influence of Specimen Geometry on Sample Disturbance Observed in Oedometric Testing of Clay Shales. Geotechnical Testing Journal, 2012, 35, 771-783.	0.5	3
63	Validation of boundary PIV measurements of soil–pipe interaction. International Journal of Physical Modelling in Geotechnics, 2011, 11, 23-32.	0.5	16
64	Effect of GCL Properties on Shrinkage When Subjected to Wet-Dry Cycles. Journal of Geotechnical and Geoenvironmental Engineering - ASCE, 2011, 137, 1019-1027.	1.5	36
65	Water-Retention Behavior of Geosynthetic Clay Liners. Journal of Geotechnical and Geoenvironmental Engineering - ASCE, 2011, 137, 1028-1038.	1.5	83
66	Characterization of Transparent Soil for Unsaturated Applications. Geotechnical Testing Journal, 2011, 34, 445-456.	0.5	17
67	Erosional control of the kinematics and geometry of foldâ€andâ€thrust belts imaged in a physical and numerical sandbox. Journal of Geophysical Research, 2010, 115, .	3.3	57
68	Three-dimensional ground displacements from static pipe bursting in stiff clay. Canadian Geotechnical Journal, 2010, 47, 439-450.	1.4	21
69	Strain localisations in FRP-confined concrete: new insights. Proceedings of the Institution of Civil Engineers: Structures and Buildings, 2009, 162, 301-309.	0.4	47
70	Ground Displacements from a Pipe-Bursting Experiment in Well-Graded Sand and Gravel. Journal of Geotechnical and Geoenvironmental Engineering - ASCE, 2009, 135, 1713-1721.	1.5	14
71	Measurement of Matric Suction Using Tensiometric and Axis Translation Techniques. Geotechnical and Geological Engineering, 2008, 26, 615-631.	0.8	70
72	Measurement of Matric Suction Using Tensiometric and Axis Translation Techniques. , 2008, , 3-19.		2

#	Article	IF	CITATIONS
73	Crack initiation in clay observed in beam bending. Geotechnique, 2007, 57, 581-594.	2.2	72
74	Quantifying geomembrane wrinkles using aerial photography and digital image processing. Geosynthetics International, 2007, 14, 219-227.	1.5	58
75	A simple displacement model for response analysis of EPS geofoam seismic buffers. Soil Dynamics and Earthquake Engineering, 2007, 27, 344-353.	1.9	31
76	A porous-matrix sensor to measure the matric potential of soil water in the field. European Journal of Soil Science, 2007, 58, 18-25.	1.8	32
77	A Case Study in Tensiometer interpretation: Centrifuge Modelling of Unsaturated Slope Behaviour. , 2006, , 2300.		7
78	Influence of a Weathered Zone on the Susceptibility of a Slope to Rainfall Induced Instability. , 2006, , 2291.		1
79	Discussion of "Accuracy of Digital Image Correlation for Measuring Deformations in Transparent Media―by Samer Sadek, Magued G. Iskander, and Jinyuan Liu. Journal of Computing in Civil Engineering, 2005, 19, 217-219.	2.5	7
80	Abridged translation of the paper from "Landslides― Evaluation of landslide triggering mechanisms in model fill slopes. W. A. Take, M. D. Bolton, P. C. P. Wong and F. J. Yeung. Journal of the Japan Landslide Society, 2005, 42, 267-268.	0.1	1
81	Evaluation of landslide triggering mechanisms in model fill slopes. Landslides, 2004, 1, 173-184.	2.7	171
82	Soil deformation measurement using particle image velocimetry (PIV) and photogrammetry. Geotechnique, 2003, 53, 619-631.	2.2	1,151
83	Tensiometer saturation and the reliable measurement of soil suction. Geotechnique, 2003, 53, 159-172.	2.2	100
84	Earth pressures on unyielding retaining walls of narrow backfill width. Canadian Geotechnical Journal, 2001, 38, 1220-1230.	1.4	127
85	Strength parameter selection framework for evaluating the design life of clay cut slopes. Proceedings of the Institution of Civil Engineers: Geotechnical Engineering, 0, , 1-20.	0.9	2